Dual sensitivity of sarcoplasmic/endoplasmic Ca^{2+}-ATPase to cytosolic and endoplasmic reticulum Ca^{2+} as a mechanism of modulating cytosolic Ca^{2+} oscillations

Kojiro YANO[1], Ole H. PETERSEN and Alexei V. TEPIKIN

The Physiological Laboratory, University of Liverpool, Crown Street, Liverpool L69 3BX, U.K.

The effects of ER (endoplasmic reticulum) Ca^{2+} on cytosolic Ca^{2+} oscillations in pancreatic acinar cells were investigated using mathematical models of the Ca^{2+} oscillations. We first examined the mathematical model of SERCA (sarcoplasmic/endoplasmic reticulum Ca^{2+}-ATPase) to reproduce the highly co-operative inhibitory effect of Ca^{2+} in the ER lumen on ER Ca^{2+} uptake in the acinar cells. The model predicts that luminal Ca^{2+} would most probably inhibit the conversion of the conformation state with luminal Ca^{2+}-binding sites (E_2) into the conformation state with cytoplasmic Ca^{2+}-binding sites (E_1). The SERCA model derived from this prediction showed dose–response relationships to cytosolic and luminal Ca^{2+} concentrations that were consistent with the experimental data from the acinar cells. According to a mathematical model of cytosolic Ca^{2+} oscillations based on the modified SERCA model, a small decrease in the concentration of endoplasmic reticulum Ca^{2+} (approx. 20 % of the total) was sufficient to abolish the oscillations. When a single type of IP_3R (IP_3 receptor) was included in the model, store depletion decreased the spike frequency. However, the frequency became less sensitive to store depletion when we added another type of IP_3R with higher sensitivity to the concentration of free Ca^{2+} in the cytosol. Bifurcation analysis of the mathematical model showed that the loss of Ca^{2+} from the ER lumen decreased the sensitivity of cytosolic Ca^{2+} oscillations to IP_3 [Ins(1,4,5)P_3]. The addition of a high-affinity IP_3R did not alter this property, but significantly decreased the sensitivity of the spike frequency to IP_3. Our mathematical model demonstrates how luminal Ca^{2+}, through its effect on Ca^{2+} uptake, can control cytosolic Ca^{2+} oscillations.

Key words: Ca^{2+} signalling, computational model, endoplasmic reticulum, pancreatic acinar cell, sarcoplasmic/endoplasmic reticulum Ca^{2+}-ATPase (SERCA).

INTRODUCTION

Cytosolic Ca^{2+} oscillation is a widespread phenomenon, found in a variety of excitable and non-excitable cells. In excitable cells, periodic changes of the plasma membrane potential can drive cytosolic Ca^{2+} oscillations by stimulating voltage-dependent Ca^{2+} channels. On the other hand, oscillations in non-excitable cells are based on periodic release of Ca^{2+} from the intracellular Ca^{2+} store and Ca^{2+} uptake into the store. The release of Ca^{2+} from the internal stores, which are mainly in the ER (endoplasmic reticulum), is mediated by Ca^{2+} channels, such as IP_3Rs {IP_3 [Ins(1,4,5)P_3] receptors} and RyRs (ryanodine receptors), in the ER membrane. Opening of the channels is regulated by cytosolic second messengers [e.g. IP_3, cADPR (cADP-ribose) and NAADP (nicotinic acid–adenine dinucleotide phosphate)]. The uptake of cytosolic Ca^{2+} into the ER, which restores $[Ca^{2+}]_c$ (concentration of free Ca^{2+} in the cytosol) to the resting level, is mediated by Ca^{2+}-ATPases located in the ER membrane [SERCAs (sarcoplasmic/endoplasmic reticulum Ca^{2+}-ATPases)].

Ca^{2+}-transport mechanisms in pancreatic acinar cells have been well characterized, and the kinetics of both cytosolic and ER Ca^{2+} have been investigated in detail by the combined use of ER-trapped fluorescent calcium indicators [1] and measurement of Ca^{2+}-dependent Cl^- current [2]. We have demonstrated previously that an incubation of acinar cells in a Ca^{2+}-free medium during Ca^{2+} oscillations caused a continuous decrease in $[Ca^{2+}]_{ER}$ (concentration of free Ca^{2+} in the ER), accompanied by a reduction of the amplitude of Ca^{2+} oscillations [3]. Ca^{2+} lost from the ER to the cytosol is excluded by PMCA (plasma membrane Ca^{2+}-ATPase), since there is rapid activation of this pump during each cytosolic Ca^{2+} spike, as demonstrated for this cell type [4]. In the acinar cells, a decrease of spike amplitude was seen as soon as store depletion became detectable. A relatively small decrease in $[Ca^{2+}]_{ER}$ [compared with the store depletion evoked by supramaximal doses of ACh (acetylcholine)] was sufficient to abolish cytosolic Ca^{2+} oscillations completely. Such phenomena imply a robust effect of Ca^{2+} in the ER lumen on cytosolic Ca^{2+} oscillations.

One of the possible mechanisms by which $[Ca^{2+}]_{ER}$ affects cytosolic Ca^{2+} oscillations is inhibition of Ca^{2+} uptake by ER Ca^{2+}. We have demonstrated previously that in intact acinar cells, an increase in $[Ca^{2+}]_{ER}$ suppressed ER Ca^{2+} uptake [2]. The inhibition by high $[Ca^{2+}]_{ER}$ was highly co-operative (Hill coefficient > 4) and the uptake rate was halved when $[Ca^{2+}]_{ER}$ was increased by approx. 50 μM. Such high co-operativity has also been shown in HL-60 cells [5] and dorsal root ganglia neurons [6]. High sensitivity of Ca^{2+} uptake to $[Ca^{2+}]_{ER}$ would allow modulation of Ca^{2+} oscillations by a relatively small decrease of $[Ca^{2+}]$

Abbreviations used: ACh, acetylcholine; cADPR, cADP ribose; $[Ca^{2+}]_c$, concentration of free Ca^{2+} in the cytosol; $[Ca^{2+}]_{ER}$, concentration of free Ca^{2+} in the endoplasmic reticulum; CCK, cholecystokinin; E_1, conformation state of sarcoplasmic/endoplasmic reticulum Ca^{2+}-ATPase with cytoplasmic high-affinity Ca^{2+}-binding sites; E_2, conformation state of sarcoplasmic/endoplasmic reticulum Ca^{2+}-ATPase with luminal low-affinity Ca^{2+}-binding sites; ER, endoplasmic reticulum; IP_3, Ins(1,4,5)P_3; IP_3R, IP_3 receptor; NAADP, nicotinic acid–adenine dinucleotide phosphate; PMCA, plasma membrane Ca^{2+}-ATPase; RyR, ryanodine receptor; SERCA, sarcoplasmic/endoplasmic reticulum Ca^{2+}-ATPase.

[1] To whom correspondence should be addressed (email vzb10326@liv.ac.uk).

in the store. The major subtype of SERCA in both pancreatic acinar cells and HL-60 cells is SERCA2b [7,8]. The activity of SERCA2b is known to be regulated by direct interaction with ER resident chaperones, including calreticulin [9,10], calnexin [11] and ERp57 [12]. The interaction between SERCA2b and the ER chaperones is sensitive to the condition of the Ca^{2+} store, suggesting that SERCA2b may respond to a change of the luminal $[Ca^{2+}]$ by using ER chaperones as ER Ca^{2+} sensors. These data indicate that the luminal sensitivity of Ca^{2+} uptake in the acinar cells and HL-60 cells reflects the property of SERCA2b.

A variety of mathematical models are available to analyse qualitative and quantitative properties of Ca^{2+} oscillations [13]. Although the stimulatory effect of cytosolic Ca^{2+} on Ca^{2+} uptake was included in most of these models, the inhibitory effect of luminal Ca^{2+} has rarely been taken into account. On the other hand, mathematical models have been developed to study the activity of SERCAs in isolated microsomes [14,15], and could reproduce the effect of luminal Ca^{2+} on the turnover rate of the pump, although the effects of luminal Ca^{2+} in these models were quantitatively different from what has been observed in pancreatic acinar cells. However, it should be possible to modify these models using experimental data from the acinar cells to obtain a mathematical model of ER Ca^{2+} uptake that can be used in Ca^{2+} oscillation models for pancreatic acinar cells.

In the present study, we first developed a mathematical model of SERCA2b to reproduce the effect of luminal Ca^{2+} on ER Ca^{2+} uptake that was seen in the pancreatic acinar cell. Then the SERCA2b model was incorporated into a computational model of cytosolic Ca^{2+} oscillations in the acinar cells. An attempt was made to reproduce the observed effect of luminal Ca^{2+} on the cytosolic Ca^{2+} oscillations by comparing the kinetics of both $[Ca^{2+}]_c$ and $[Ca^{2+}]_{ER}$ with the experimental data from the acinar cells. Thereafter bifurcation analysis was utilized to analyse the effects of luminal Ca^{2+} on the properties of cytosolic Ca^{2+} oscillations.

METHODS

Mathematical models were designed using Maple (Maplesoft, Ontario, Canada) and implemented in SIMULINK (The Mathworks, Natick, MA, U.S.A.). The flux control coefficients in the kinetic model of SERCA were calculated using GEPASI [16]. All the bifurcation analyses were carried out using XPPAUT [17].

RESULTS

Kinetic models of SERCAs

The kinetic models for the reaction cycle of SERCAs were based on the model developed by Dode et al. [14]. In this model, the reversible catalytic cycle was composed of the following reactions (see Figure 1A): (1) binding of two Ca^{2+} to the SERCA pump from the cytoplasmic side of the ER membrane, (2) phosphorylation of the pump by ATP, (3) conversion from the E_1 (cytoplasmic high-affinity Ca^{2+}-binding sites) into the E_2 (luminal low-affinity Ca^{2+}-binding sites) conformation state and translocation of Ca^{2+} from the cytoplasmic side to the luminal side of the ER membrane, (4) release of Ca^{2+} into the ER lumen, (5) dephosphorylation of the pump and (6) conversion from the E_2 into the E_1 conformation state. All the reactions are described as first-order reactions (except for the binding of Ca^{2+}).

Since the model of Dode et al. [14] was based on experimental data relating to SERCA1a, we needed to adjust the parameters to reproduce the property of SERCA2b in pancreatic acinar cells. It has been shown that SERCA2b sensitivity to cytosolic Ca^{2+} is higher than for SERCA1a $\{K_{a,0.5}$ (half maximum activation by cytosolic $Ca^{2+}) = 0.27\ \mu M$ and $0.44\ \mu M$ respectively, when expressed in COS cells [18]$\}$. Therefore we increased the affinity for cytosolic Ca^{2+} in reaction 1 from $1.79\ \mu M$ to $1.1\ \mu M$. The data from HL-60 and pancreatic acinar cells suggest that luminal Ca^{2+} can inhibit ER Ca^{2+} uptake, both at high and low cytosolic Ca^{2+} concentrations [2,5]. On the other hand, the data from Dode et al. [14] indicate that the effect of luminal Ca^{2+} on SERCA1a is much more predominant at high $[Ca^{2+}]_c$. This difference in the

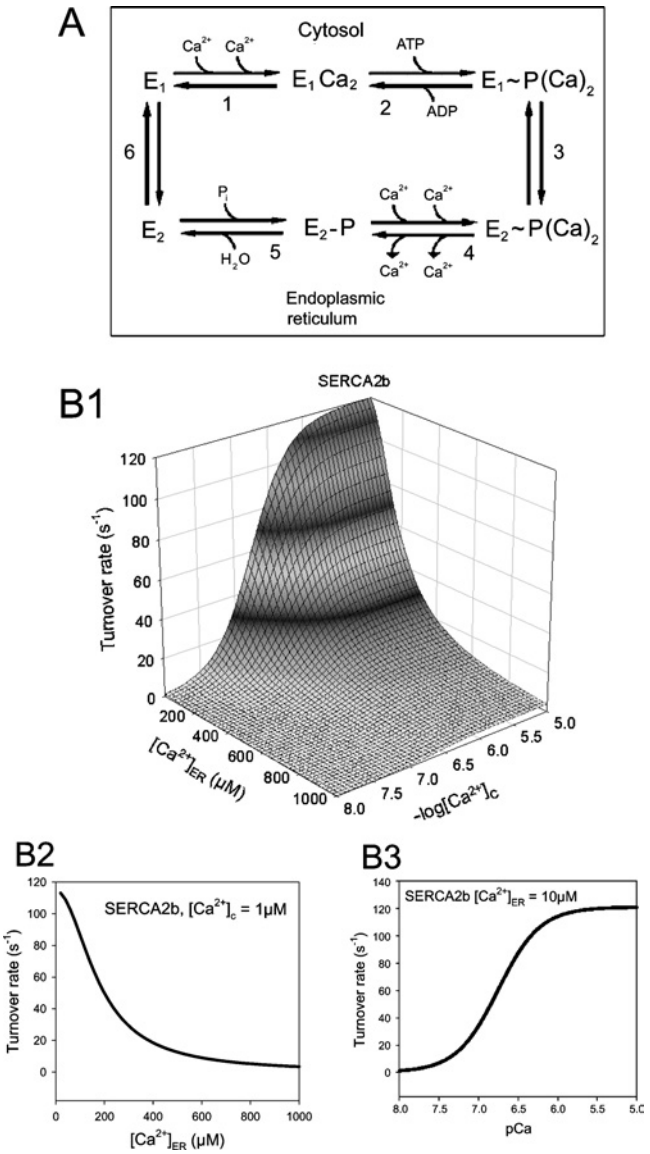

Figure 1 Reaction cycle and dose–response of turnover rate to cytosolic and luminal Ca^{2+} in SERCA2b model

(**A**) Reaction cycle of SERCA. Clockwise direction of a reaction in the cycle is defined as a 'forward' reaction. The numbers shown with the reactions are used in the text in order to refer to individual reactions. (**B1**) Estimated dose–response of the turnover rate of SERCA2b against $[Ca^{2+}]_c$ and $[Ca^{2+}]_{ER}$. Note that $[Ca^{2+}]_c$ is expressed on a logarithmic scale and $[Ca^{2+}]_{ER}$ is on a linear scale (this representation is chosen for visual convenience). (**B2**) Turnover rate at different $[Ca^{2+}]_{ER}$ when $[Ca^{2+}]_c = 1\ \mu M$. (**B3**) Turnover rate at different $[Ca^{2+}]_c$ when $[Ca^{2+}]_{ER} = 10\ \mu M$.

Table 1 Flux control coefficients of turnover rate of SERCA1a model

$[Ca^{2+}]_{ER}$ was fixed at 100 μM.

Reaction	Flux control coefficients (forward/backward)	
	$[Ca^{2+}]_c = 100$ nM	$[Ca^{2+}]_c = 10$ μM
3	$3.15 \times 10^{-2}/-1.67 \times 10^{-3}$	$2.11 \times 10^{-1}/-1.11 \times 10^{-2}$
4	$2.14 \times 10^{-2}/-2.23 \times 10^{-3}$	$1.43 \times 10^{-1}/-1.46 \times 10^{-2}$
5	$3.86 \times 10^{-2}/-9.73 \times 10^{-4}$	$2.53 \times 10^{-1}/-4.75 \times 10^{-4}$
6	$4.59 \times 10^{-1}/-4.30 \times 10^{-1}$	$2.24 \times 10^{-1}/-2.56 \times 10^{-2}$

Table 2 Rate constants for the kinetic model of SERCA2b

Reaction numbers refer to Figure 1. c, $[Ca^{2+}]_c$; e, $[Ca^{2+}]_{ER}$.

Reaction	Rate constants (s^{-1})	
	Forward	Backward
1	$5000 \times c^{1.65}/(c^{1.65} + 1.1^{1.65})$	10
2	700	5
3	600	50
4	1000	$13\,580 \times e^2/(e^2 + 1550^2)$
5	500	1
6	$4.64 \times 10^6/(e^2 + 87.4^2)$	600

relationship between cytoplasmic Ca^{2+} and luminal Ca^{2+} indicates that SERCA2b responds to luminal Ca^{2+} using a mechanism that is distinct from that employed by SERCA1a.

We hypothesized that there is another reaction in the cycle that is affected by luminal Ca^{2+}. The reaction should affect the turnover rate to a similar degree at both low and high $[Ca^{2+}]_c$ in order to be consistent with the above observation in the acinar cell. The strength of the effect resulting from a change of the rate constant of a local reaction v_i (e.g. an individual reaction in the catalytic cycle of SERCA) on the global flux J (e.g. the turnover rate of the pump) can be quantified as

$$C(J,i) = (\partial J/J)/(\partial v_i/v_i)$$

where $(\partial J/J)$ is the fractional change of the global flux, $(\partial v_i/v_i)$ is the fractional change of the rate constant of the local reaction and $C(J,i)$ is the ratio of the fractional changes, called flux control coefficient [19]. By calculating the control coefficients of the individual steps in the catalytic cycle of SERCA, we can determine which step has the greatest potential to influence the overall turnover rate. It has been shown that, when a parameter (such as $[Ca^{2+}]_{ER}$) acts on the global flux through its direct influence on a local reaction, the strength of the response of the global flux to the parameter (or response coefficient) is determined by the control coefficient of the local reaction multiplied by the strength of the response of the local reaction to the parameter (or elasticity) [19]. Therefore a sufficient response of the global flux to the parameter can be achieved only at a reaction step that has a sufficiently large flux control coefficient.

We assumed that the luminal Ca^{2+} could only affect the E_2 conformation and, therefore, only the control coefficients for the reactions that involve E_2 were calculated (Table 1). In the majority of cases, forward reactions had larger control coefficients than backward reactions, which would be expected if the forward reactions were dominant at the steady state. A cytosolic Ca^{2+} rise from 100 nM to 10 μM increased the control coefficients (except for reaction 6) approx. 10-fold, which may explain why luminal Ca^{2+} has a larger effect at higher concentrations of cytosolic Ca^{2+}. The forward direction of reaction 6 ($E_2 \rightarrow E_1$ conversion) had the highest control coefficient at a cytosolic Ca^{2+} concentration of 100 nM among the reactions in the catalytic cycle, which was relatively insensitive to cytosolic Ca^{2+} changes. This suggests that the $E_2 \rightarrow E_1$ conversion is most likely to be responsible for the sensitivity of ER Ca^{2+} uptake to luminal Ca^{2+} in HL-60 and pancreatic acinar cells.

For estimation of the parameters, we assumed that SERCA1a and SERCA2b would show the same property (except for the sensitivity to cytosolic Ca^{2+}) when the store was empty. On the other hand, an increase in $[Ca^{2+}]_{ER}$ would inhibit the $E_2 \rightarrow E_1$ conversion with a Hill coefficient of 2. The dose-dependency of the turnover rate against $[Ca^{2+}]_{ER}$ at $[Ca^{2+}]_c = 100$ nM was fitted to the data from [2] to obtain the apparent affinity of the pump to luminal Ca^{2+}. This gave us the SERCA2b kinetic model, whose estimated dose–response curves against $[Ca^{2+}]_c$ and $[Ca^{2+}]_{ER}$ are shown in Figure 1(B1). The rate constants of the reactions are shown in Table 2.

Figure 1(B1) shows that the turnover rate of SERCA2b was inhibited strongly by luminal Ca^{2+} both at low and high cytosolic $[Ca^{2+}]$, which is in agreement with the experiments performed in pancreatic acinar and HL-60 cells. With $[Ca^{2+}]_c = 1$ μM, the turnover rate was 114.3 s^{-1} at $[Ca^{2+}]_{ER} = 10$ μM and 3.28 s^{-1} at $[Ca^{2+}]_{ER} = 1$ mM, and $K_{i,0.5}$ (half maximum inhibition by luminal Ca^{2+}) = 176 μM (Figure 1B2). The estimated $K_{i,0.5}$ was close to the resting $[Ca^{2+}]_{ER}$ in the pancreatic acinar cell (approx. 150 μM [20]). The $K_{a,0.5}$ was 0.18 μM (Figure 1B3, $[Ca^{2+}]_{ER} =$ 10 μM).

Effect of $[Ca^{2+}]_{ER}$ and SERCA activity on cytosolic Ca^{2+} oscillations in the whole-cell model

We constructed a 'whole-cell model' for Ca^{2+} oscillations in pancreatic acinar cells. This whole-cell model was composed of two compartments: the cytoplasm and the ER. The model included the following transport mechanisms: (i) Ca^{2+} release from the store via IP_3Rs, (ii) Ca^{2+} leak from the store, (iii) Ca^{2+} extrusion by PMCA, (iv) Ca^{2+} uptake by SERCA2b. The details of the transport mechanisms are given in the Appendix.

Figure 2(A) shows Ca^{2+} spike changes during continuous Ca^{2+} extrusion without compensation by Ca^{2+} influx through the plasma membrane. This would correspond to the experimental observation of cytosolic Ca^{2+} oscillations with no external Ca^{2+}. Ca^{2+} oscillations were initiated by an increase of $[IP_3]$ from 0 to 0.254 μM at $t = 0$. In the model, the amplitudes of the cytosolic Ca^{2+} responses decreased as $[Ca^{2+}]_{ER}$ decreased, and oscillations eventually disappeared at $[Ca^{2+}]_{ER} = 160$ μM. The periods between the spikes gradually increased as the store depletion progressed. We could see an increase in both rise time (time from the base to the peak of the next spike, 8.9 s in the first spike and 17.1 s in the last spike), and decay time (the spike period minus the rise time, 6.7 s in the first spike and 15.2 s in the last) (Figure 2B).

In order to learn more about the mechanism of spike modulation by luminal Ca^{2+}, we carried out bifurcation analysis. Figure 3(A) shows a typical shape of a bifurcation curve for IP_3-induced Ca^{2+} oscillations. The diagram displays $[Ca^{2+}]_c$ at different $[IP_3]$. At low and high $[IP_3]$, $[Ca^{2+}]_c$ does not oscillate, and the diagram shows the steady state $[Ca^{2+}]_c$ (solid lines). At an intermediate $[IP_3]$, $[Ca^{2+}]_c$ oscillates and the diagram shows the maximum (peak) and the minimum (baseline) $[Ca^{2+}]_c$ (broken lines). Therefore this diagram is showing the range of $[IP_3]$ which gives

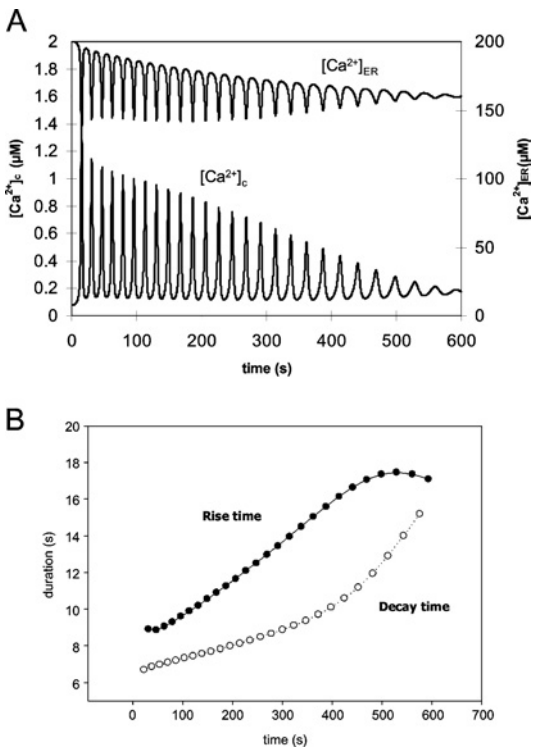

Figure 2 Simulation of cytosolic Ca^{2+} oscillations in a pancreatic acinar cell during gradual store depletion

The gradual depletion of the Ca^{2+} store in the model was achieved by the extrusion of cytosolic Ca^{2+} by PMCA and the lack of compensating Ca^{2+} influx through the plasma membrane. (**A**) $[Ca^{2+}]_c$ (lower trace) and $[Ca^{2+}]_{ER}$ (upper trace) during the simulation. At the resting condition $[Ca^{2+}]_c = 0.08\ \mu M$ and $[Ca^{2+}]_{ER} = 200\ \mu M$. The cell was stimulated by increasing $[IP_3]$ from 0 to 0.254 μM. (**B**) The rise time (●) and the decay time (○) of cytosolic Ca^{2+} spikes during the simulation.

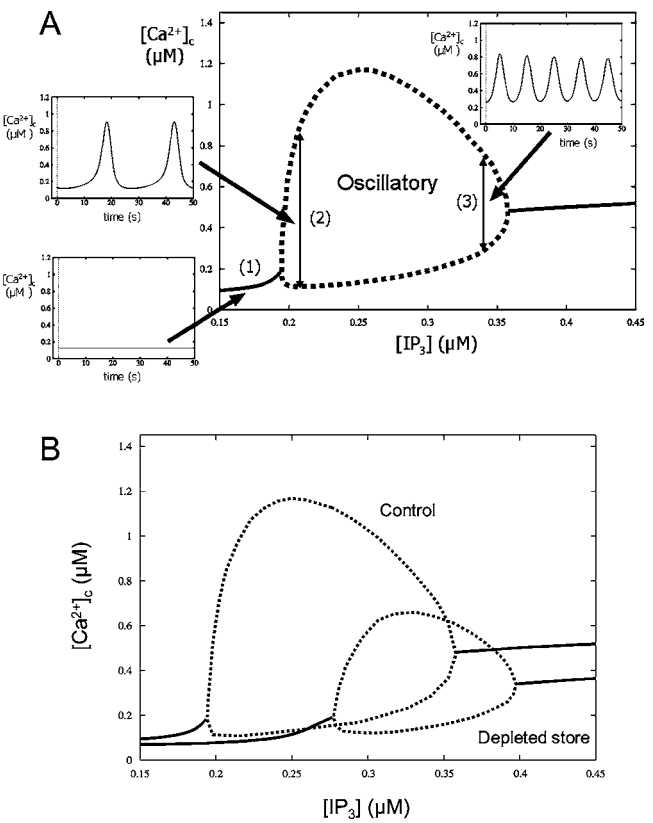

Figure 3 Bifurcation analysis of the modifications of Ca^{2+} oscillations by store depletion

(**A**) A typical bifurcation diagram of $[Ca^{2+}]_c$ against $[IP_3]$ in IP_3-induced Ca^{2+} oscillations is presented. Steady-state solutions (solid line) and the maxima and the minima of $[Ca^{2+}]_c$ during Ca^{2+} oscillations (broken line) are shown. $[Ca^{2+}]_c$ will be stationary when $[IP_3]$ is outside the 'oscillatory' area (1). $[Ca^{2+}]_c$ oscillates when $[IP_3]$ is in the 'oscillatory' area, which is encompassed by the broken line (2 and 3). Oscillation frequency is faster at higher $[IP_3]$ (3) than lower $[IP_3]$ (2). (**B**) Bifurcation diagrams of $[Ca^{2+}]_c$ against $[IP_3]$ in the whole-cell model. Steady-state solutions (solid line), the maxima and the minima of $[Ca^{2+}]_c$ during Ca^{2+} oscillations (broken line) are shown. $S = 200\ \mu M$ in control and $S = 160\ \mu M$ in depleted store.

oscillations as well as the range of $[Ca^{2+}]_c$ when it is oscillatory.

Figure 3(B) shows the bifurcation diagram of cytosolic Ca^{2+} in the whole-cell model with $[IP_3]$ as a bifurcation parameter. A decrease of S (resting $[Ca^{2+}]_{ER}$ at $[Ca^{2+}]_c = 0.08\ \mu M$) from 200 μM to 160 μM decreased the maximum oscillation amplitude of the oscillations by 0.515 μM (from 1.05 μM to 0.535 μM), but did not abolish the oscillations. It also raised both the minimum and maximum $[IP_3]$ for Ca^{2+} oscillations from $[IP_3]_{min} = 0.196\ \mu M$, $[IP_3]_{max} = 0.358\ \mu M$ ($S = 200\ \mu M$) to $[IP_3]_{min} = 0.278\ \mu M$, $[IP_3]_{max} = 0.397\ \mu M$ ($S = 160\ \mu M$). This shift of the bifurcation curve towards higher $[IP_3]$ can be interpreted as 'desensitization' of Ca^{2+} response to IP_3, because a higher $[IP_3]$ will be required to obtain Ca^{2+} oscillations when the store is depleted.

Multiple subtypes of IP_3R may decrease the sensitivity of spike frequency to store depletion

Although store depletion has normally been observed to decrease both spike frequency and amplitudes, there are some cases with little frequency change, even when the spike amplitude was reduced strongly due to store depletion [3,4,21]. Since minor parameter modifications in our whole-cell model failed to reproduce such stability of spike frequency, we decided to incorporate an extra mechanism in the model: an additional subtype of the IP_3R. It has been shown that there are at least three distinct subtypes (types 1, 2 and 3) of IP_3R in mammalian cells, including pancreatic acinar cells [22,23]. The proportion of the IP_3R subtypes varies between cell types [23], and it has been suggested that changes in this proportion can affect cytosolic Ca^{2+} signals [24,25]. The properties of the IP_3R subtypes differ in many ways, including the sensitivity to activation by cytosolic Ca^{2+} [26,27] and IP_3 [25,28], inhibition by cytosolic Ca^{2+} [29,30], and susceptibility to phosphorylation by protein kinase A [31].

We included in our whole-cell model the sensitivity difference between the IP_3R subtypes to activation by cytosolic Ca^{2+} and that was sufficient to reproduce the behaviour of spike frequency when the store was depleted. It has been suggested that the type-3 IP_3R plays the major role in the generation of agonist-induced cytosolic Ca^{2+} oscillations in pancreatic acinar cells [31,32]. However, the type-2 IP_3R, which has a higher affinity for cytosolic Ca^{2+} than the type-3 IP_3R [25,27,29], could also contribute to Ca^{2+} oscillations. Significant levels of expression of the type-2 IP_3R subtype were observed in the pancreas [23,33], whereas the level of the type-1 IP_3R is reported to be low [23] and unlikely to contribute to the Ca^{2+} signalling in this cell type. In order to model the heterogeneous expressions of IP_3R subtypes qualitatively, we incorporated an IP_3R with higher affinity for cytosolic Ca^{2+} in

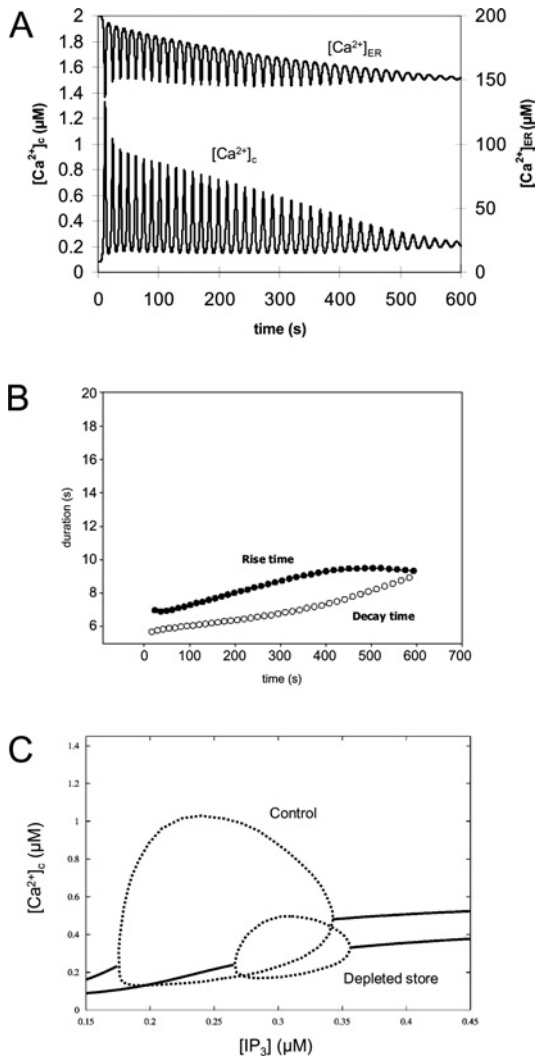

Figure 4 Simulation of cytosolic Ca^{2+} oscillations in a pancreatic acinar cell during gradual store depletion when two subtypes of IP_3R are present

The store was depleted gradually in the same way as in Figure 2. (**A**) $[Ca^{2+}]_c$ (lower trace) and $[Ca^{2+}]_{ER}$ (upper trace) in the whole-cell model with two subtypes of IP_3R. In this simulation, it was assumed that the 'high-affinity' IP_3R subtype had three times higher affinity to cytosolic Ca^{2+} than the subtype used for the simulation in Figure 2. (**B**) The rise time (●) and the decay time (○) of Ca^{2+} spikes during the simulation. (**C**) Bifurcation diagrams of $[Ca^{2+}]_c$ against $[IP_3]$ in the whole-cell model. Steady-state solutions (solid line), the maxima and the minima of periodic orbits (broken line) are shown. $S = 200\ \mu M$ in control and $S = 160\ \mu M$ in depleted store.

the whole-cell model, in addition to the IP_3R used in the previous model. Figure 4(A) shows Ca^{2+} spike changes during continuous Ca^{2+} extrusion without Ca^{2+} influx through the plasma membrane. As before, store depletion decreased the spike amplitude and abolished spiking at $[Ca^{2+}]_{ER}$ of approx. $150\ \mu M$, which was slightly lower than in the whole-cell model with a single type of IP_3R. Rise time (from 6.5 s to 10.7 s) and decay time (from 5.7 s to 9.0 s) (Figure 4B) also increased, but the magnitude of the changes was smaller than in the simulation based on a single IP_3R. This effect of a high-affinity IP_3R on the stability of spike frequency was seen only when its contribution to Ca^{2+} release was relatively small (20 % of total release in the example shown in Figure 4A) and having a larger proportion of high-affinity IP_3R inhibited Ca^{2+} oscillations (results not shown).

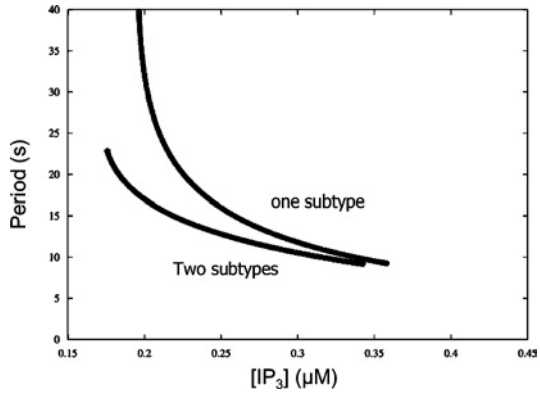

Figure 5 Relationship between $[IP_3]$ and oscillation periods when one or two IP_3R subtypes were present

The traces compare the relationship between the period of cytosolic Ca^{2+} oscillations and $[IP_3]$ in the mathematical models with one and two subtypes of IP_3R.

Figure 4(C) shows the bifurcation diagram of cytosolic Ca^{2+}. The decrease of S (resting $[Ca^{2+}]_{ER}$ at $[Ca^{2+}]_c = 0.08\ \mu M$) from $200\ \mu M$ to $160\ \mu M$ decreased the maximum amplitudes of the oscillations by $0.571\ \mu M$ (from 0.897 to $0.326\ \mu M$) and shifted the curve to higher $[IP_3]$ ($[IP_3]_{min} = 0.176\ \mu M$, $[IP_3]_{max} = 0.342\ \mu M$ with $S = 200\ \mu M$; $[IP_3]_{min} = 0.266\ \mu M$, $[IP_3]_{max} = 0.356\ \mu M$ with $S = 160\ \mu M$). The extent of the amplitude changes of the oscillations and the curve shift were comparable with that of the whole-cell model with a single IP_3R subtype. This suggests that the co-expression of two IP_3R subtypes did not significantly alter the basic property of the inhibition of Ca^{2+} oscillations by store depletion. However, co-expression seems to affect the sensitivity of the Ca^{2+} spike frequency to $[IP_3]$. Figure 5 shows the spike period at different $[IP_3]$. When only a single IP_3R was expressed, a decrease in $[IP_3]$ increased the spike period rapidly and went beyond 40 s at the lowest possible $[IP_3]$ for sustainable Ca^{2+} oscillations. The spike period in the model with two IP_3R subtypes was similar compared with the single IP_3R system when $[IP_3]$ was high, but was much smaller when $[IP_3]$ was low.

DISCUSSION

In the present study, we have developed a mathematical model for SERCA2b, and analysed the effect of the ER luminal Ca^{2+} on cytosolic Ca^{2+} oscillations. Using data for the relationship between $[Ca^{2+}]_{ER}$ and ER Ca^{2+} uptake rate in intact pancreatic acinar cells [2], as well as kinetic data from isolated ER vesicles [14,18], we have produced a portrait of the dual dependence of SERCA2b activity on cytosolic and ER Ca^{2+} as a three-dimensional plot. Our SERCA2b model is based on prediction from the flux control coefficients of the mathematical model for SERCA1a, indicating that there should be an additional effect of luminal Ca^{2+} on SERCA2b that inhibits ER Ca^{2+} uptake at low $[Ca^{2+}]_c$. Our mathematical model of SERCA is more complete than previously published models [14,15], because it reproduces accurately not only the sensitivity of ER Ca^{2+} uptake to luminal Ca^{2+} in the acinar cells, but also modulation of this sensitivity by cytosolic Ca^{2+}, which was not addressed by previous models. Khan et al. [34] showed that a $[Ca^{2+}]_{ER}$ rise increased the phosphorylation level of SERCAs by P_i. As a high concentration of P_i alone was not sufficient for maximum phosphorylation,

they suggested that there must be binding sites for luminal Ca^{2+} in an unphosphorylated form. Therefore the effect of luminal Ca^{2+} would be shifting the equilibrium from E_1 to E_2 that was subsequently phosphorylated by P_i in their experiments. This is consistent with our hypothesis that the conversion from E_2 into E_1 is sensitive to luminal Ca^{2+}.

In the computational models, store depletion decreased both the amplitude and frequency of cytosolic Ca^{2+} oscillations. In bifurcation diagrams, store depletion raised both the lower and higher thresholds of $[IP_3]$ and 'desensitized' Ca^{2+} oscillations to $[IP_3]$. It has been shown experimentally that the spike frequency and amplitude are positively correlated to $[IP_3]$ in pancreatic acinar cells [35] and, therefore, this shift of the bifurcation curve would decrease both amplitude and frequency of Ca^{2+} oscillations. It may appear to be counter-intuitive that an increase of ER Ca^{2+} uptake stimulated by store depletion prolonged the decay time, as these two events are often considered to be negatively correlated [36,37]. This puzzling relationship between ER Ca^{2+} uptake rate and decay time is associated with the decrease of spike amplitude caused by store depletion. When the amplitude is smaller, the feedback inhibition of Ca^{2+} release by cytosolic Ca^{2+} and the stimulation of Ca^{2+} uptake by store depletion will be weaker. In this situation, both rise and decay times will become longer. The pattern of change in spike shapes during gradual store depletion in our model is consistent with the change during ACh-induced slow Ca^{2+} spikes (period > 100 s) in the pancreatic acinar cell with decreased external Ca^{2+} [4].

Spike amplitudes decrease with constant spike frequency during gradual store Ca^{2+} depletion. This was observed both with regard to ACh-induced fast oscillations [3] and CCK (cholecystokinin)-induced slow oscillations in pancreatic acinar cells [4,38]. In the mathematical model, it is possible to enhance the stability of spike frequency by co-expressing two subtypes of IP_3R. Therefore ACh and CCK may also be utilizing more than one release mechanism to generate Ca^{2+} oscillations. Pancreatic acinar cells have all three subtypes of IP_3R [23], as well as cADPR- [39] and NAADP- [40] mediated release mechanisms, which are strongly linked to the RyR [41].The interaction between these Ca^{2+}-release mechanisms is crucial for the generation of the spatial and temporal patterns of Ca^{2+} oscillations [42]. Changes in CCK concentration have much smaller effects on the frequency of Ca^{2+} oscillations than on the amplitude [43], which supports our model in which the spike frequency is stable when Ca^{2+} oscillations are governed by multiple Ca^{2+}-release mechanisms. However, if the frequency is controlled by oscillations in the concentration of the Ca^{2+}-releasing second messenger, store depletion would also decrease amplitude without affecting its frequency [44]. Such a mechanism has not been demonstrated in pancreatic acinar cells, where application of second messengers through a patch pipette is sufficient to cause Ca^{2+} oscillations [42]. However, oscillations of the messenger concentration cannot be ruled out in some types of agonist-induced Ca^{2+} oscillations.

Since the rate of Ca^{2+} release from the ER should depend on the concentration gradient of Ca^{2+} across the ER membrane, $[Ca^{2+}]_{ER}$ can also affect Ca^{2+} release. Caroppo et al. [45] reported recently that the extent of IP_3-induced Ca^{2+} release, assessed by changes in the fluorescence of ER-trapped Mag-fura-2, was dependent on the luminal Ca^{2+} concentration. Falcke et al. [46] also showed that the overexpression of SERCA2b in *Xenopus* oocytes elevated $[Ca^{2+}]_{ER}$ and increased the amplitude of Ca^{2+} oscillations. By comparing the experimental results with mathematical models, Falcke et al. [46] suggested that the enhancement of Ca^{2+} release caused by the elevation of $[Ca^{2+}]_{ER}$ could offset the inhibitory effect of the increased Ca^{2+} uptake. Since only the IP_3R was sensitive to the luminal Ca^{2+} in their mathematical model, their results indicate that $[Ca^{2+}]_{ER}$ can modulate cytosolic Ca^{2+} oscillations in *Xenopus* oocytes through its effect on the IP_3R when the Ca^{2+} uptake is insensitive to luminal Ca^{2+}. If the rate of Ca^{2+} release is proportional to the Ca^{2+} concentration gradient between the ER and the cytosol, $[Ca^{2+}]_{ER}$ would affect Ca^{2+} release much less than Ca^{2+} uptake, since $[Ca^{2+}]_{ER}$ can inhibit Ca^{2+} uptake with high co-operativity. Instead, luminal Ca^{2+} may alter the open probability of Ca^{2+}-release channels in a non-linear fashion by direct or indirect interactions with the channels.

Recently, Sneyd et al. [47] examined the relationship between cytosolic Ca^{2+} oscillations and plasma membrane Ca^{2+} influx both theoretically and experimentally. They argued, using mathematical models, that the total cellular Ca^{2+} during steady state Ca^{2+} oscillations can be lower than in the resting condition and just above the threshold level to maintain cytosolic Ca^{2+} oscillations. In this condition, the loss of cellular Ca^{2+} during a Ca^{2+} spike due to Ca^{2+} extrusion by PMCA would need to be recovered by Ca^{2+} entry from the plasma membrane in the inter-spike period before the next Ca^{2+} rise. Therefore blockage of Ca^{2+} influx during steady-state Ca^{2+} oscillations will keep the total Ca^{2+} below the threshold and thereby acutely abolish the oscillations. They supported this concept by showing experimentally that blockade of Ca^{2+} influx and efflux by La^{3+} during carbachol-induced Ca^{2+} oscillations could acutely block cytosolic Ca^{2+} oscillations in HEK-293 cells. The difference between their model and ours, in which the removal of external Ca^{2+} reduced Ca^{2+} spike amplitudes only gradually, can be explained by the difference in the kinetics of the Ca^{2+} oscillations observed. While we modelled relatively fast Ca^{2+} oscillations (period of approx. 10 s), Sneyd et al. [47] examined slow Ca^{2+} oscillations (period of approx. 100 s) in which each Ca^{2+} spike will be accompanied by significant Ca^{2+} extrusion. Park et al. [3] observed small, but detectable, decreases of $[Ca^{2+}]_{ER}$ (approx. 20 μM) during each slow Ca^{2+} oscillation spike. In this case, the recovery of $[Ca^{2+}]_{ER}$ would depend on Ca^{2+} influx. No such changes in $[Ca^{2+}]_{ER}$ were observed during fast Ca^{2+} oscillation spikes. This suggests that, during the fast oscillations, the decrease in Ca^{2+} influx from the plasma membrane will not have an immediate effect on $[Ca^{2+}]_{ER}$. Therefore the effect of blocking Ca^{2+} influx observed by Sneyd et al. [47] is not directly applicable to our model. Nevertheless, it is remarkable that a small decrease in $[Ca^{2+}]_{ER}$, during an inter-spike period, can be sufficient to abolish Ca^{2+} oscillations, and this suggests that SERCA2b, known to be present in HEK-293 cells [48], may have a strong luminal sensitivity in this cell type, exactly as in the acinar cell.

Using computational models, we analysed the effect of changes in $[Ca^{2+}]_{ER}$ on Ca^{2+} oscillations in pancreatic acinar cells. Our SERCA2b model successfully reproduced the highly non-linear inhibition of ER Ca^{2+} uptake by luminal Ca^{2+} in this cell type and demonstrated the dual dependence of Ca^{2+} uptake on $[Ca^{2+}]_c$ and $[Ca^{2+}]_{ER}$. In the whole-cell model, we observed a high sensitivity of the amplitude of cytosolic Ca^{2+} oscillations to changes in $[Ca^{2+}]_{ER}$ that was consistent with the experimental finding [3]. A whole-cell model with a single IP_3R type did not reproduce the ability of Ca^{2+} oscillations to retain the spike frequency when the amplitude was being reduced by store depletion. However, we have found that the inclusion of an additional subtype of IP_3R with higher affinity to cytosolic Ca^{2+} enhanced the stability of spike frequency during store depletion, suggesting a co-operative effect between the IP_3R subtypes. We expect that our mathematical models will advance understanding of the regulation of Ca^{2+} oscillations by cytosolic and luminal Ca^{2+}.

We thank Nina Burdakova and Mark Houghton for technical assistance. K. Y. is a Wellcome Trust Prize Ph.D. student.

APPENDIX

The structure of the whole-cell model

The differential equations for $[Ca^{2+}]$ in the cytosol (c) and the endoplasmic reticulum (e) were:

$$dc/dt = J_{re} + J_{leak} - J_{SERCA} - J_{PMCA}$$
$$de/dt = C_b(-J_{re} - J_{leak} + J_{SERCA})$$

where C_b is the ratio of the Ca^{2+}-buffering capacities of the cytosol and the ER, J_{re} is the Ca^{2+}-release rate from the IP_3R, J_{leak} is the Ca^{2+}-leak rate from the ER, J_{SERCA} is the Ca^{2+}-uptake rate by SERCA and J_{PMCA} is the Ca^{2+}-extrusion rate by PMCA.

Ca^{2+} uptake by SERCA

Turnover rates were calculated from the kinetic models of SERCA2b and converted into uptake rate by multiplying them by conversion factors (V_p).

Ca^{2+} release from IP_3R

We used the mathematical model of Ca^{2+} waves in pancreatic acinar cells of Sneyd et al. [49] for the IP_3R model. This model assumed three states of the receptor (shut, open or inactive) where $[IP_3]$ and $[Ca^{2+}]_c$ regulate the transit of the states. The differential equations for the probability of three states (x for shut, y for open and z for inactive state) were:

$$dx/dt = \varphi_{-1}(c)y - p\varphi_1(c)x + \varphi_3(c)z$$
$$dy/dt = p\varphi_1(c)x - \varphi_{-1}(c)y + \varphi_2(c)y$$
$$z = 1 - x - y$$

where $\varphi_1(c) = (k_1R_1 + r_2c)/(R_1 + c)$, $\varphi_{-1}(c) = (k_{-1} + r_{-2})R_3/(c + R_3)$, $\varphi_2(c) = (k_2R_3 + r_4c)/(R_3 + c)$, $\varphi_3(c) = (k_3R_5 + r_6c)/(R_5 + c)$ and $P(c) = y^4$.

$$J_{re} = K_f P(c)(e - c)$$

where p is $[IP_3]$, $P(c)$ is open probability and K_f is the maximum Ca^{2+} release rate from the IP_3R.

Ca^{2+} extrusion by PMCA

The rate of Ca^{2+} extrusion from the cytosol by the plasma membrane in a pancreatic acinar cell was measured as described by Camello et al. [50] using the droplet technique. We derived an empirical relationship between cytosolic Ca^{2+} and the extrusion rate from the measurements:

$$J_{PMCA} = V_{pm} \times c^2 / \left(c^2 + K_{pm}{}^2\right)$$

Table A1 Parameters for the whole-cell model of Ca^{2+} oscillations in pancreatic acinar cells

Parameter	Value (unit)	Parameter	Value (unit)
K_f	54 ($\mu M \cdot s^{-1}$)	r_6	0
k_1	0	R_1	6 (μM)
k_{-1}	0.88 (s^{-1})	R_3	50 (μM)
k_2	0.53 (s^{-1})	R_5	1.6 (μM)
k_3	1 (s^{-1})	J_{leak}	0.2 ($\mu M \cdot s^{-1}$)
r_2	100 (s^{-1})	V_p	0.0257 (μM)
r_{-2}	0	V_{pm}	0.0028 ($\mu M \cdot s^{-1}$)
r_4	20 (s^{-1})	K_{pm}	0.23 (μM)

where V_{pm} is the maximum extrusion rate and K_{pm} is the apparent affinity of PMCA to cytosolic Ca^{2+}.

Ca^{2+} leak from the ER

It has been shown that the leak rate does not change significantly when $[Ca^{2+}]_{ER}$ is above 100 μM [2]. Therefore J_{leak} was set to be constant in the whole-cell model.

All the parameter values for the whole-cell model are summarized in Table A1. These values were used in all the simulations unless otherwise stated.

REFERENCES

1 Hofer, A. M., Landolfi, B., Debellis, L., Pozzan, T. and Curci, S. (1998) Free $[Ca^{2+}]$ dynamics measured in agonist-sensitive stores of single living intact cells: a new look at the refilling process. EMBO J. **17**, 1986–1995

2 Mogami, H., Tepikin, A. V. and Petersen, O. H. (1998) Termination of cytosolic Ca^{2+} signals: Ca^{2+} reuptake into intracellular stores is regulated by the free Ca^{2+} concentration in the store lumen. EMBO J. **17**, 435–442

3 Park, M. K., Petersen, O. H. and Tepikin, A. V. (2000) The endoplasmic reticulum as one continuous Ca^{2+} pool: visualization of rapid Ca^{2+} movements and equilibration. EMBO J. **19**, 5729–5739

4 Tepikin, A. V., Voronina, S. G., Gallacher, D. V. and Petersen, O. H. (1992) Pulsatile Ca^{2+} extrusion from single pancreatic acinar cells during receptor-activated cytosolic Ca^{2+} spiking. J. Biol. Chem. **267**, 14073–14076

5 Favre, C. J., Schrenzel, J., Jacquet, J., Lew, D. P. and Krause, K. H. (1996) Highly supralinear feedback inhibition of Ca^{2+} uptake by the Ca^{2+} load of intracellular stores. J. Biol. Chem. **271**, 14925–14930

6 Solovyova, N., Veselovsky, N., Toescu, E. C. and Verkhratsky, A. (2002) Ca^{2+} dynamics in the lumen of the endoplasmic reticulum in sensory neurons: direct visualization of Ca^{2+}-induced Ca^{2+} release triggered by physiological Ca^{2+} entry. EMBO J. **21**, 622–630

7 Favre, C. J., Jerstrom, P., Foti, M., Stendhal, O., Huggler, E., Lew, D. P. and Krause, K. H. (1996) Organization of Ca^{2+} stores in myeloid cells: association of SERCA2b and the type-1 inositol-1,4,5-trisphosphate receptor. Biochem. J. **316**, 137–142

8 Lee, M. G., Xu, X., Zeng, W., Diaz, J., Kuo, T. H., Wuytack, F., Raeymaekers, L. and Muallem, S. (1997) Polarized expression of Ca^{2+} pumps in pancreatic and salivary gland cells: role in initiation and propagation of $[Ca^{2+}]_i$ waves. J. Biol. Chem. **272**, 15771–15776

9 Camacho, P. and Lechleiter, J. D. (1995) Calreticulin inhibits repetitive intracellular Ca^{2+} waves. Cell **82**, 765–771

10 John, L. M., Lechleiter, J. D. and Camacho, P. (1998) Differential modulation of SERCA2 isoforms by calreticulin. J. Cell Biol. **142**, 963–973

11 Roderick, H. L., Lechleiter, J. D. and Camacho, P. (2000) Cytosolic phosphorylation of calnexin controls intracellular Ca^{2+} oscillations via an interaction with SERCA2b. J. Cell Biol. **149**, 1235–1248

12 Li, Y. and Camacho, P. (2004) Ca^{2+}-dependent redox modulation of SERCA 2b by ERp57. J. Cell Biol. **164**, 35–46

13 Sherman, A. S., Li, Y. and Keizer, J. E. (2002) Whole-cell models. In Computational Cell Biology (Fall, C. P., Marland, E. S., Wagner, J. M. and Tyson, J. J., eds.), pp. 101–139, Springer-Verlag, New York

14 Dode, L., Vilsen, B., Van Baelen, K., Wuytack, F., Clausen, J. D. and Andersen, J. P. (2002) Dissection of the functional differences between sarco(endo)plasmic reticulum Ca^{2+}-ATPase (SERCA) 1 and 3 isoforms by steady-state and transient kinetic analyses. J. Biol. Chem. **277**, 45579–45591

15 Inesi, G. and de Meis, L. (1989) Regulation of steady state filling in sarcoplasmic reticulum: roles of back-inhibition, leakage, and slippage of the calcium pump. J. Biol. Chem. **264**, 5929–5936

16 Mendes, P. (1993) GEPASI: a software package for modelling the dynamics, steady states and control of biochemical and other systems. Comput. Appl. Biosci. **9**, 563–571

17 Ermentrout, B. (2002) Simulating, Analyzing and Animating Dynamical Systems: A Guide to XPPAUT for Researchers and Students, SIAM, Philadelphia

18 Lytton, J., Westlin, M., Burk, S. E., Shull, G. E. and MacLennan, D. H. (1992) Functional comparisons between isoforms of the sarcoplasmic or endoplasmic reticulum family of calcium pumps. J. Biol. Chem. **267**, 14483–14489

19 Fell, D. A. (1997) Metabolic control analysis. In Understanding the Control of Metabolism, pp. 101–134, Portland Press, London

20 Park, M. K., Tepikin, A. V. and Petersen, O. H. (1999) The relationship between acetylcholine-evoked Ca^{2+}-dependent current and the Ca^{2+} concentrations in the cytosol and the lumen of the endoplasmic reticulum in pancreatic acinar cells. Pflügers Arch. **438**, 760–765

21 Shuttleworth, T. J. and Thompson, J. L. (1996) Ca^{2+} entry modulates oscillation frequency by triggering Ca^{2+} release. Biochem. J. **313**, 815–819
22 Lee, M. G., Xu, X., Zeng, W., Diaz, J., Wojcikiewicz, R. J., Kuo, T. H., Wuytack, F., Raeymaekers, L. and Muallem, S. (1997) Polarized expression of Ca^{2+} channels in pancreatic and salivary gland cells: correlation with initiation and propagation of $[Ca^{2+}]_i$ waves. J. Biol. Chem. **272**, 15765–15770
23 Wojcikiewicz, R. J. (1995) Type I, II, and III inositol 1,4,5-trisphosphate receptors are unequally susceptible to down-regulation and are expressed in markedly different proportions in different cell types. J. Biol. Chem. **270**, 11678–11683
24 Hattori, M., Suzuki, A. Z., Higo, T., Miyauchi, H., Michikawa, T., Nakamura, T., Inoue, T. and Mikoshiba, K. (2004) Distinct roles of inositol 1,4,5-trisphosphate receptor types 1 and 3 in Ca^{2+} signaling. J. Biol. Chem. **279**, 11967–11975
25 Miyakawa, T., Maeda, A., Yamazawa, T., Hirose, K., Kurosaki, T. and Iino, M. (1999) Encoding of Ca^{2+} signals by differential expression of IP_3 receptor subtypes. EMBO J. **18**, 1303–1308
26 Boehning, D. and Joseph, S. K. (2000) Functional properties of recombinant type I and type III inositol 1,4,5-trisphosphate receptor isoforms expressed in COS-7 cells. J. Biol. Chem. **275**, 21492–21499
27 Ramos-Franco, J., Fill, M. and Mignery, G. A. (1998) Isoform-specific function of single inositol 1,4,5-trisphosphate receptor channels. Biophys. J. **75**, 834–839
28 Wojcikiewicz, R. J. and Luo, S. G. (1998) Differences among type I, II, and III inositol-1,4,5-trisphosphate receptors in ligand-binding affinity influence the sensitivity of calcium stores to inositol-1,4,5-trisphosphate. Mol. Pharmacol. **53**, 656–662
29 Mak, D. O., McBride, S. and Foskett, J. K. (2001) Regulation by Ca^{2+} and inositol 1,4,5-trisphosphate ($InsP_3$) of single recombinant type 3 $InsP_3$ receptor channels. Ca^{2+} activation uniquely distinguishes types 1 and 3 $InsP_3$ receptors. J. Gen. Physiol. **117**, 435–446
30 Swatton, J. E. and Taylor, C. W. (2002) Fast biphasic regulation of type 3 inositol trisphosphate receptors by cytosolic calcium. J. Biol. Chem. **277**, 17571–17579
31 Giovannucci, D. R., Groblewski, G. E., Sneyd, J. and Yule, D. I. (2000) Targeted phosphorylation of inositol 1,4,5-trisphosphate receptors selectively inhibits localized Ca^{2+} release and shapes oscillatory Ca^{2+} signals. J. Biol. Chem. **275**, 33704–33711
32 Straub, S. V., Giovannucci, D. R., Bruce, J. I. and Yule, D. I. (2002) A role for phosphorylation of inositol 1,4,5-trisphosphate receptors in defining calcium signals induced by peptide agonists in pancreatic acinar cells. J. Biol. Chem. **277**, 31949–31956
33 Fujino, I., Yamada, N., Miyawaki, A., Hasegawa, M., Furuichi, T. and Mikoshiba, K. (1995) Differential expression of type 2 and type 3 inositol 1,4,5-trisphosphate receptor mRNAs in various mouse tissues: *in situ* hybridization study. Cell Tissue Res. **280**, 201–210
34 Khan, Y. M., East, J. M. and Lee, A. G. (1997) Effects of pH on phosphorylation of the Ca^{2+}-ATPase of sarcoplasmic reticulum by inorganic phosphate. Biochem. J. **321**, 671–676
35 Wakui, M., Potter, B. V. and Petersen, O. H. (1989) Pulsatile intracellular calcium release does not depend on fluctuations in inositol trisphosphate concentration. Nature (London) **339**, 317–320
36 Camacho, P. and Lechleiter, J. D. (1993) Increased frequency of calcium waves in *Xenopus laevis* oocytes that express a calcium-ATPase. Science **260**, 226–229
37 Majewska, A., Brown, E., Ross, J. and Yuste, R. (2000) Mechanisms of calcium decay kinetics in hippocampal spines: role of spine calcium pumps and calcium diffusion through the spine neck in biochemical compartmentalization. J. Neurosci. **20**, 1722–1734
38 Yule, D. I. and Williams, J. A. (1992) U73122 inhibits Ca^{2+} oscillations in response to cholecystokinin and carbachol but not to JMV-180 in rat pancreatic acinar cells. J. Biol. Chem. **267**, 13830–13835
39 Thorn, P., Gerasimenko, O. and Petersen, O. H. (1994) Cyclic ADP-ribose regulation of ryanodine receptors involved in agonist evoked cytosolic Ca^{2+} oscillations in pancreatic acinar cells. EMBO J. **13**, 2038–2043
40 Cancela, J. M., Churchill, G. C. and Galione, A. (1999) Coordination of agonist-induced Ca^{2+}-signalling patterns by NAADP in pancreatic acinar cells. Nature (London) **398**, 74–76
41 Gerasimenko, J. V., Maruyama, Y., Yano, K., Dolman, N. J., Tepikin, A. V., Petersen, O. H. and Gerasimenko, O. V. (2003) NAADP mobilizes Ca^{2+} from a thapsigargin-sensitive store in the nuclear envelope by activating ryanodine receptors. J. Cell Biol. **163**, 271–282
42 Cancela, J. M., Van Coppenolle, F., Galione, A., Tepikin, A. V. and Petersen, O. H. (2002) Transformation of local Ca^{2+} spikes to global Ca^{2+} transients: the combinatorial roles of multiple Ca^{2+} releasing messengers. EMBO J. **21**, 909–919
43 Tsunoda, Y., Stuenkel, E. L. and Williams, J. A. (1990) Oscillatory mode of calcium signaling in rat pancreatic acinar cells. Am. J. Physiol. **258**, C147–C155
44 Hirose, K. and Iino, M. (1994) Heterogeneity of channel density in inositol-1,4,5-trisphosphate-sensitive Ca^{2+} stores. Nature (London) **372**, 791–794
45 Caroppo, R., Colella, M., Colasuonno, A., DeLuisi, A., Debellis, L., Curci, S. and Hofer, A. M. (2003) A reassessment of the effects of luminal $[Ca^{2+}]$ on inositol 1,4,5-trisphosphate-induced Ca^{2+} release from internal stores. J. Biol. Chem. **278**, 39503–39508
46 Falcke, M., Li, Y., Lechleiter, J. D. and Camacho, P. (2003) Modeling the dependence of the period of intracellular Ca^{2+} waves on SERCA expression. Biophys. J. **85**, 1474–1481
47 Sneyd, J., Tsaneva-Atanasova, K., Yule, D. I., Thompson, J. L. and Shuttleworth, T. J. (2004) Control of calcium oscillations by membrane fluxes. Proc. Natl. Acad. Sci. U.S.A. **101**, 1392–1396
48 Poch, E., Leach, S., Snape, S., Cacic, T., MacLennan, D. H. and Lytton, J. (1998) Functional characterization of alternatively spliced human SERCA3 transcripts. Am. J. Physiol. **275**, C1449–C1458
49 Sneyd, J., LeBeau, A. and Yule, D. I. (2000) Traveling waves of calcium in pancreatic acinar cells: model construction and bifurcation analysis. Phys. D **145**, 158–179
50 Camello, P., Gardner, J., Petersen, O. H. and Tepikin, A. V. (1996) Calcium dependence of calcium extrusion and calcium uptake in mouse pancreatic acinar cells. J. Physiol. **490**, 585–593

Received 15 April 2004/28 June 2004; accepted 20 July 2004
Published as BJ Immediate Publication 20 July 2004, DOI 10.1042/BJ20040629